Chiang Mai J. Sci. 2018; 45(4) : 1835-1842
http://epg.science.cmu.ac.th/ejournal/
Contributed Paper

Quantitative Phase Analysis and Crystal Structure of DyBCO Ceramics Prepared at Different Sintering Conditions

Paitoon Boonsong [a,b], Pimpilai Wannasut [a,b], Ampika Rachakom [c] and Anucha Watcharapasorn* [a,d]

[a] Department of Physics and Materials Science, Faculty of Science, Chiang Mai University, Chiang Mai 50200, Thailand.

[b] Graduate School, Chiang Mai University, Chiang Mai 50200, Thailand.

[c] Science branch, Faculty of Science and Agricultural Technology, Rajamangala University of Technology Lanna, Chiang Mai 50300, Thailand.

[d] Materials Science Research Center, Faculty of Science, Chiang Mai University, Chiang Mai 50200, Thailand.

* Author for correspondence; e-mail: anucha@stanfordalumni.org

Received: 22 February 2017
Accepted: 18 April 2017

ABSTRACT

The DyBCO ceramics were fabricated by solid-state reaction method under a normal air atmosphere using a stoichiometric amount (i.e. Dy:Ba:Cu = 1:2:3) of high-purity Dy_2O_3, $BaCO_3$ and CuO starting powders, which were previously mixed and calcined at 900°C for 4 h. The green DyBCO pellets were sintered at various sintering temperatures (i.e. 850, 900, 930, 950 and 980°C) for 2 h. The influence of sintering process on phase formation of ceramics was observed by X-ray diffraction (XRD). The quantitative phase analysis of ceramics was analyzed by fitting the XRD pattern using the PowderCell program. The results showed that the $DyBa_2Cu_3O_{7-\beta}$ composition was identified as the main crystalline phase. At higher temperatures (> 950°C), the Dy_2BaCuO_5 (Dy-211) secondary phase was observed. The relative fraction of various phases was discussed in relation to phase formation and density change. The SEM-EDS/WDS images of ceramics exhibited irregular shaped grains. The average grain size increased from ~2.3 to ~7.0 μm when the sintering temperature was increased. The possibility of stoichiometric change in DyBCO ceramic due to different processing conditions was also discussed in details.

Keywords: $DyBa_2Cu_3O_{7-\beta}$, sintering, ceramic, quantitative phase analysis, crystal structure

1. INTRODUCTION

$ReBa_2Cu_3O_{7-\beta}$ or Re-123 (Re = rare earth element such as Y, Nd, Sm, Eu, Gd, Dy, Ho, Er) material is known as a high-T_c superconductor whose properties are suitable for high-field electronic applications such as power cable, magnetic bearing, fault current limiter and permanent magnet [1-3]. On the other hand, Pr-123 is a compound

iso-structural to the Re-123 group but non-superconducting. Theoretical models such as hole filling [4-6], hole localization in CuO_2 plane [7-11] and magnetic pair breaking [12-14] have been used to explain the suppression of T_c and superconducting-insulator transition in this compound in addition to the role of oxygen deficiency in CuO chains which induces the orthorhombic-tetragonal phase transition at its critical temperature [15]. This shows that, in this Re-123 series, a wide range of electrical conduction behavior can be tuned by chemical variation and defect formation. Studies in the past have suggested that the Re-123 (Re = Nd, Sm, Eu, Gd, Dy, etc.) have better applicability compared to $YBa_2Cu_3O_{7-\beta}$ (Y-123) system [16-19]. They show higher transition temperatures, better surface morphology and better performance under external magnetic fields. It is well known that Dy-123 (DyBCO) is an oxide compound whose crystal structure is composed of rocksalt and perovskite units. When prepared in air, this compound seemed to have better electronic-tuning ability compared to that of Y-123 system [16-19].

The electrical conduction of Re-123 is known to be dependent on oxygen content and this behavior has previously been evaluated by mathematical methods based on the electronic structure of Y-123 phase [24]. It has also been suggested that the oxygen concentration is somewhat related to c-axis parameter. For Dy-123, similar studies on the relationship between electronic structures, oxygen stoichio-metry, crystallographic data and processing conditions were quite scarce. Therefore, in this work, the influence of different sintering temperatures on the fabrication of pure DyBCO ceramics using the solid-state reaction method was investigated. By employing quantitative phase analysis, the relation of phase formation with crystal-structure and microstructural changes, composition and physical properties such as density and mean grain size was discussed in details.

2. MATERIALS AND METHODS

DyBCO ceramics were fabricated by the solid-state reaction and sintering method. The DyBCO powder was prepared using high-purity Dy_2O_3, $BaCO_3$ and CuO starting powders. The powders were mixed in a stoichiometric ratio of Dy : Ba : Cu = 1 : 2 : 3 and ball milled for 24 h in polyethylene jar with zirconia balls as milling media. The mixed powders were dried and calcined in an opened alumina crucible at 900°C for 4 h under normal atmosphere. The heating/ cooling rate used was 5°C/min. The phase of calcined powder (DyBCO) was confirmed by X-ray diffraction technique (XRD). The DyBCO powder was reground and sieved for homogeneous size distribution. It was then pressed into disc-shape pellets and sintered at 850, 900, 930 and 980°C for 2 h under a normal air atmosphere with heating/ cooling rates of 5°C/min. The apparent density of the ceramics was measured by the Archimedes method using xylene as the liquid medium. The theoretical value of density was calculated using the chemical composition and unit cell size from quantitative analysis based on experimental XRD patterns and PowderCell 2.4 program [20]. Phase formation of the ceramics was investigated by XRD (Phillips Xpert pro Diffractometer). The relative volume fraction of phases present in DyBCO ceramics was also calculated using a quantitative analysis based on experimental XRD patterns and PowderCell 2.4 program [20]. The microstructure of ceramics was observed using a scanning electron microscope (SEM: JEOL, JSM591OLV) and chemical composition identification was carried out

using energy dispersive X-ray spectroscopy analysis (SEM-EDS). The quantitative analysis of individual elements was confirmed using wavelength dispersive X-ray spectrometry (WDS) (SEM: JEOL, JSM-IT300).

3. RESULTS AND DISCUSSION

The XRD patterns of the DyBCO powder and the DyBCO ceramics are shown in Figure 1. In all cases, the desired $DyBa_2Cu_3O_{7-\beta}$ (Dy-123) phase was identified as the main crystalline phase. The XRD pattern of the DyBCO powder corresponded well with the $DyBa_2Cu_3O_{6.84}$ phase (JCPDS file no. 01-079-0047), indicating an orthorhombic perovskite structure with the space group Pmmm. This was confirmed by its simulated XRD pattern as shown in Figure 2 and relevant data are also listed in Table 1. The morphology of DyBCO powder exhibited irregular shape with particle size ~ 1-2 μm and atomic percentage ratio of Dy : Ba : Cu: O was about 7.32 : 15.90 : 23.02 : 53.76 (see Table 2), hence, resulting in an approximated composition of $DyBa_{2.17}Cu_{3.14}O_{7.32}$. After sintering process, the diffraction peaks shifted slightly to lower angles. For example, the DyBCO ceramic sintered at 950°C for 2 h showed the diffraction peak shift of (112), (200) and (213) reflections from 2θ angles of 32.77° to 32.63°, 46.72° to 46.56° and 58.23° to 57.11°, respectively. This could be because the structure slightly expanded. It was possible that the loss of oxygen ions from the lattice could change the valence of cation, for example, from smaller Cu^{2+} to larger Cu^{1+} as reported by Krabbes et al. [21] which in turn could induce the observed change in unit cell volume. The XRD analysis of the sample sintered at 980°C had high background noise. This noise may have contribution from uneven distribution of large particles (Dy_2BaCuO_5 (Dy-211) phase) as well as the presence of amorphous phase (frozen Ba-Cu-O liquid phase). Hence, the simulated pattern could not be reliably produced.

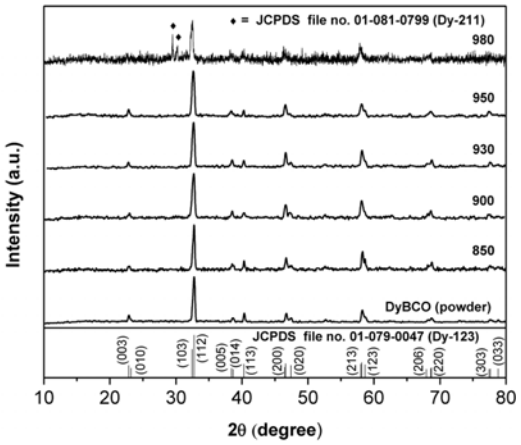

Figure 1. XRD patterns of the DyBCO powder and ceramics sintered at various temperatures.

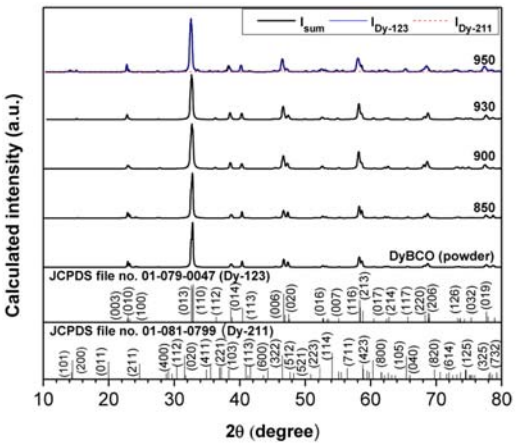

Figure 2. Simulated XRD patterns of the DyBCO powder and ceramics sintered at various temperatures.

Table 1. Lattice parameters, density, relative density, shrinkage and weight loss of DyBCO powder and ceramic samples sintered at various temperatures.

Sample	Dy-123				Density	Relative	Shrinkage	Weight
	a (Å)	b (Å)	c (Å)	V (Å^3)	(g/cm^3)	density (%)	(%)	loss (%)
powder	3.838	3.891	11.638	170.088	-	-	-	-
850	3.837	3.892	11.637	173.793	5.25	74.91	1.14	1.61
900	3.840	3.900	11.655	174.517	6.54	93.32	9.50	1.94
930	3.833	3.874	11.674	173.330	6.55	93.46	9.38	1.48
950	3.842	3.884	11.704	174.676	6.61	93.80	11.27	2.02
980	-	-	-	-	6.44	-	8.34	3.97

Table 2. Evaluated elemental composition of the DyBCO ceramics.

sintering (°C)	Evaluated elemental composition (at. %)							
	EDS				WDS			
	Dy	Ba	Cu	O	Dy	Ba	Cu	O
powder	7.32	15.90	23.02	53.76	-	-	-	-
850	11.81	24.52	30.49	33.17	-	-	-	-
900	10.85	24.02	34.13	38.77	9.60	20.39	26.78	43.25
930	10.04	22.04	29.14	38.58	9.08	21.43	27.62	41.88
950	2.57	31.20	33.65	32.58	10.53	23.64	34.19	31.63
980	13.40	22.36	33.26	30.98	-	-	-	-

The quantitative analysis of XRD results indicated that the ceramic samples sintered at temperatures below 950°C showed pure Dy-123 phase with orthorhombic perovskite structure. The unit cell dimensions of the DyBCO samples obtained from XRD analysis data were listed in Table 1. Studies in the past have suggested that the oxygen content can be calculated from the change in c-axis value of the unit cell [22-24]. It could be noticed that the c-axis value of orthorhombic structure increased when the sintering temperatures increased. The increase of c-axis value tended to be accompanied by the reduction of oxygen content in DyBCO ceramics. This trend was similar to the result of the unit cell parameters of the Re-123 (Re = Y, Er, Gd, etc) as a function of the oxygen content [22-24]. This showed that the change in orthorhombic perovskite structure was attributed to a larger oxygen deficiency. The DyBCO ceramics sintered at 950°C for 2 h contained a small amount of Dy_2BaCuO_5 (Dy-211) secondary phase which is a non-superconducting phase and its X-ray peaks corresponded to the standard data JCPDS file no. 01-081-0799 indicating an orthorhombic perovskite structure. The relative volume fraction of Dy-123 phase in this sample can be estimated using equation [25],

$$\text{Dy-123} = \Sigma\left(\frac{I_{Dy\text{-}123}}{I_{Dy\text{-}123} + I_{Dy\text{-}211}}\right) \times 100\% \quad (1)$$

where I is the peak intensity of the observed phases. The quantitative phase analysis showed that the volume fraction of the sintered ceramics at 950°C were

Dy-123 : Dy-211 = 96.39 : 3.61 vol% and the unit cell dimensions of Dy-211 were calculated to be a = 12.320, b = 5.639 and c = 7.266 Å. At high temperatures, the Dy-211 phase could form due to the peritectic decomposition of Dy-123 [26]. The Dy-123/ Dy-211 mixture was reported to have enhanced critical current density (J_c) while the amount of cracks was reduced by the presence of Dy-211 [3, 27]. The chemical reaction of the peritectic decomposition can normally be described by following equation [26]:

$$2(\text{Dy-123}) = \text{Dy-211} + Ba_3Cu_5O_8(l) + 3O_2 \quad (2)$$

This liquid phase (l) of $Ba_3Cu_5O_8$ ($3BaCuO_2 + 2CuO$) infiltrating into the porous regions increased the densification rate of ceramic samples. Figure 4 shows that the density and shrinkage of the DyBCO ceramics increased with sintering temperature and reached its maximum relative density of 93.80 % of its theoretical value at 950°C. At 980°C, the sample could not be calculated for its relative density due to partial melting and high weight loss (see Table 1).

The microstructure of the DyBCO ceramics sintered at 800, 900, 930, 950 and 980°C for 2 h are shown in Figure 3. It was found that most samples exhibited irregular shaped grains with a mean size range of 2.33-7.00 μm. Figure 5 shows the mean grain size of the DyBCO sintered at various sintering temperatures. At higher temperatures of 900°C and 930°C, (Figures 3(b)-(c)), grain growth was observed but the grain shape was nearly the same. Most of the grains presented a typical elongated form with a mean size of 4.29 ± 0.62 and 3.74 ± 0.59 μm, respectively. It seemed that the densification behavior of the ceramics sintered at 900 and 930°C were similar. The ceramic sample sintered at 950°C for 2 h showed that the measurement of grain size was difficult because the liquid phase was observed due to the peritectic decomposition. Nevertheless, this sample exhibited irregular shaped grains with an average size around 5.62 ± 1.31 μm (Figure 3(d)). At the highest sintering temperature of 980°C, the ceramic sample began to melt and the microstructure exhibited square grain shape with a mean size value of about 7.00 ± 1.33 μm (Figure 3(e)) with large pores as similarly reported by Andreouli et al. [1]. This had an effect of lowering the sample density as shown in Table 1. Table 2 shows the elemental analysis using SEM-EDS of the sintered ceramic. The results showed that the nominal composition was $DyBa_{2.08}Cu_{2.58}O_{2.81}$, $DyBa_{2.21}Cu_{3.15}O_{3.57}$ and $DyBa_{2.20}Cu_{2.90}O_{3.84}$ for the ceramics sintered at 850, 900 and 930°C, respectively. These compositions were different from the superconducting phase Dy-123 partly due to the measurement error of EDS technique. For the ceramic sintered at 950°C, the liquid phase of DyBCO ceramics (Figures 3(d)-(e)) scattered electron beams such that the EDS spectra of the ceramic samples gave higher compositional variation. The ceramics sintered at 900, 930 and 950°C were subjected to WDS measurement. The result showed that the compositions were $DyBa_{2.12}Cu_{2.79}O_{4.5}$, $DyBa_{2.36}Cu_{3.04}O_{4.6}$ and $DyBa_{2.25}Cu_{3.25}O_3$, respectively. These formulae were similar to those obtained by EDS measurement but the oxygen content showed slightly greater values. Based on these investigations, this showed that the oxygen deficiency played a role in structural change and microstructural formation accompanying the processing temperature dependence in this material system.

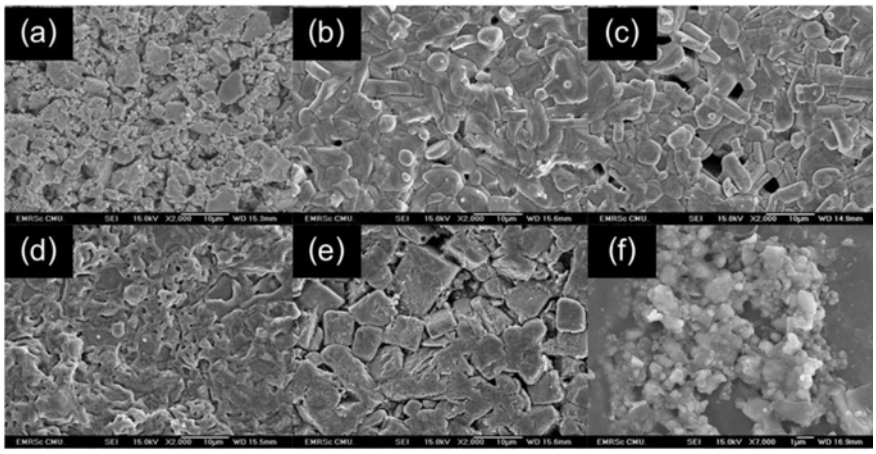

Figure 3. SEM micrographs of DyBCO ceramics sintered at (a) 800 , (b) 900, (c) 930, (d) 950 (e) 980°C for 2 h and (f) the DyBCO powder calcined at 900°C for 4 h.

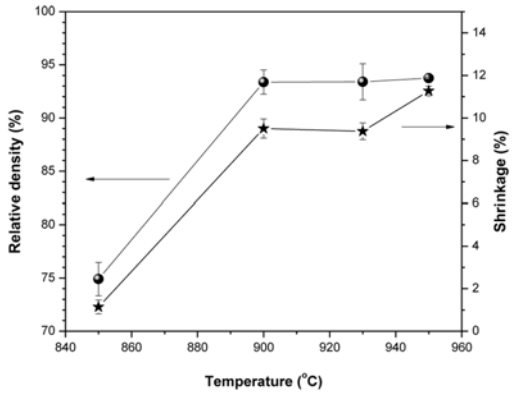

Figure 4. Relative density and shrinkage of DyBCO ceramics sintered at various sintering temperatures.

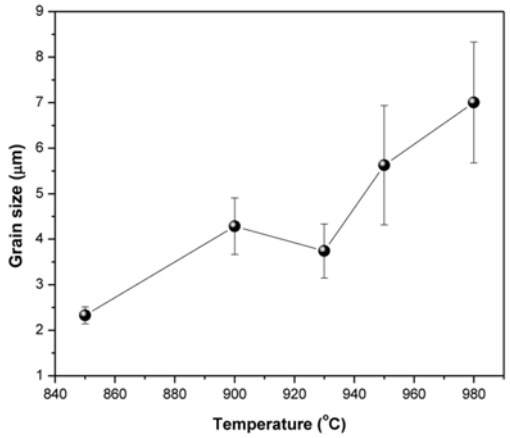

Figure 5. Mean grain size of the DyBCO ceamics sintered at various sintering temperatures.

4. CONCLUSION

The pure $DyBa_2Cu_3O_{7-\beta}$ ceramics were prepared by solid-state reaction method under normal atmosphere. In all cases, the $DyBa_2Cu_3O_{7-\beta}$ phase was identified as the main crystalline phase. At 950°C, the maximum relative density was about 93.80 % of the theoretical value. However, at 980°C, the Dy-211 phase partly formed due to peritectic decomposition of Dy-123. Crystal structure change was observed with increasing the sintering temperatures. Oxygen stoichiometric change was also observed based on the lattice dimensional variation and approximated composition from EDS and WDS data. Its deviation from Dy-123 composition seemed to largely affect the structural transformation of this material system.

ACKNOWLEDGEMENT

This research was supported by a Science Achievement Scholarship of Thailand (SAST) and instrument analysis support was given by CMU. Partial support from the Thailand Research Fund (RSA5880005 and IRG5780013), Center of Excellence in Materials Science and Materials Technology, Faculty of Science and the Graduate School, Chiang Mai University are also acknowledged.

REFERENCES

[1] Andreouli C. and Tsetsekou A., *Eur. Ceram. Soc.*, 2000; **20**: 2101-2114. DOI 10.1016/S0955-2219(00)00074-1.

[2] Skalcle J.M.S., *Mater. Sci. Eng.*, 1998; **R23**: 1-40. DOI 10.1016/S0927-796X(98) 00010-2.

[3] Nariki S. and Murakami M., *Supercond. Sci. Technol.*, 2002; **15**: 786-790. DOI 10.1088/ 0953-2048/15/5/329.

[4] Gonçalves A.P., Santos I.C., Lopes E.B., Henriques R.T., Almeida M. and Figueiredo M.O., *Phys. Rev. B*, 1988; **37**: 7476-7481. DOI 10.1103/PhysRevB.37. 7476.

[5] Kebede A., Jee C.S., Schwegler J., Crow J.E., Mihalisin T., Myer G.H., Salomon R.E., Schlottmann P., Kuric M.V., Bloom S.H. and Guertin R.P., *Phys. Rev. B*, 1989; **40**: 4453-4462. DOI 10.1103/PhysRevB.40.4453.

[6] Matsuda A., Kinoshita K., Ishii T., Shibata H., Watanabe T. and Yamada T., *Phys. Rev. B*, 1988; **38**: 2910-2913. DOI 10.1103/PhysRevB.38.2910.

[7] Tang X.X., Manthiram A. and Goodenough J.B., *Physica C*, 1989; **161**: 574-580. DOI 10.1016/0921-4534(89) 90392-4.

[8] Wei P., Ying H.W. and Qi Z.Q., *Physica C*, 1993; **209**: 400-406. DOI 10.1016/0921-4534(93)90552-2.

[9] Fehrenbacher R. and Rice T.M., *Phys. Rev. Lett.*, 1993; **70**: 3471-3474. DOI 10.1103/PhysRevLett.70.3471.

[10] Lee M., Stutzman M.L., Suzuki Y. and Geballe T.H., *Phys. Rev. B*, 1996; **54**: 3776-3779. DOI 10.1103/PhysRevB.54. R3776.

[11] Kao H.C.I., Yu F.C. and Guan W., *Physica C*, 1997; **292**: 53-58. DOI 10.1016/ S0921-4534(97)01723-1.

[12] Neumeier J.J., Bernholm T., Maple M.B. and Schuller I.K., *Phys. Rev. Lett.*, 1989; **63**: 2516-2519. DOI 10.1103/PhysRev Lett.63.2516.

[13] Tomkowicz A., Szytula A. and Wojciechowski K., *Supercond. Sci. Technol.*, 1992; **5**: 373-375. DOI 10.1088/0953-2048/5/6/009.

[14] Murugesan M., Ishigaki T. and Kuwano H., *J. Appl. Phys.*, 1999; **86**: 6985-6992. DOI 10.1063/1.371783.

[15] Jorgensen J.D., Beno M.A., Hinks D.G., Soderholm L., Volin K.J., Hitterman R.L., Grace J.D., Schuller I.K., Segre C.U., Zhang K. and Kleefish M.S., *Phys. Rev. B*, 1987; **36**: 3608-3616. DOI 10.1103/ PhysRevB.36.3608.

[16] Jia Q.X., Maiorov B., Wang H., Lin Y., Foltyn S.R., Civale L. and MacManus-Driscoll J.L., *IEEE Trans. Appl. Supercond.*, 2005; **15**: 2723-2726. DOI 10.1109/ TASC.2005.847797.

[17] MacManus-Driscoll J.L., Foltyn S.R., Jia Q.X., Wang H., Serquis A., Maiorov B., Civale L., Lin Y., Hawley M.E., Maley M.P. and Peterson D.E., *Appl. Phys. Lett.*, 2004; **84**: 5329-5331. DOI 10.1063/1.1766394.

[18] Civale L., Maiorov B., Serquis A., Willis J.O., Coulter J.Y., Wang H., Jia Q.X., Arendt P.N., MacManus-Driscoll J.L., Maley M.P. and Foltyn S.R., *Appl. Phys. Lett.*, 2004; **84**: 2121-2123. DOI 10.1063/1.1655707.

[19] Zhou H., Maiorov B., Wang H., MacManus-Driscoll J.L., Holesinger T.G., Civale L., Jia Q.X. and Foltyn S.R., *Supercond. Sci. Technol.*, 2008; **21(2)**: 025001. DOI 10.1088/0953-2048/21/ 02/025001.

[20] Kraus W. and Nolze G., *J. Appl. Cryst.*, 1996; **29**: 301-303. DOI 10.1107/S0021889895014920.

[21] Krabbes G., Fuchs G., Canders W.R., May H. and Palka R., Fundamentals; in Krabbes G., Fuchs G., Canders W.R., May H. and Palka R., eds., *High Temperature Superconductor Bulk Materials*, WILEY-VCH Verlag GmbH & Co. KGaA, Weinheim, 2006: 1-30.

[22] Prayoonphokkharat P., Jiansirisomboon S. and Watcharapasorn A., *Electron. Mater. Lett.*, 2013; **9(4)**: 413-416. DOI 10.1007/s13391-013-0020-6.

[23] Stoyanova-Ivanova A., Georgieva S.T., Nedeltcheva T., Dimova L. and Shivachev B., *Bulgarian Chem. Commun.*, 2011; **43(2)**: 320-324.

[24] Benzi P., Bottizzo E. and Rizzi N., *J. Cryt. Growth*, 2004; **269**: 625-629. DOI 10.1016/j.jcrysgro.2004.05.082.

[25] Hamadneh I., *Electron. Mater. Lett.*, 2014; **10(3)**: 597-600. DOI 10.1007/s13391-013-3250-8.

[26] Tanaka H., Narika S., Sakai N., Hirabayashi I., Murakami M. and Takizawa T., *Physica C*, 2005; **426-431**: 660-665. DOI 10.1016/j.physc.2005.02.068.

[27] Nariki S., Sakai N., Murakami M. and Hirabayashi I., *Physica C*, 2004; **412-414**: 651-656. DOI *1*0.1016/j.physc.2004.01.084.